

---

*This copy is for your personal, non-commercial use only.*

---

If you wish to distribute this article to others, you can order high-quality copies for your colleagues, clients, or customers by [clicking here](#).

Permission to republish or repurpose articles or portions of articles can be obtained by following the guidelines [here](#).

**The following resources related to this article are available online at [www.sciencemag.org](http://www.sciencemag.org) (this information is current as of October 28, 2010):**

A correction has been published for this article at:  
<http://www.sciencemag.org/cgi/content/full/sci;329/5991/512-b>

Updated information and services, including high-resolution figures, can be found in the online version of this article at:  
<http://www.sciencemag.org/cgi/content/full/328/5984/1382>

Supporting Online Material can be found at:  
<http://www.sciencemag.org/cgi/content/full/328/5984/1382/DC1>

A list of selected additional articles on the Science Web sites **related to this article** can be found at:  
<http://www.sciencemag.org/cgi/content/full/328/5984/1382#related-content>

This article **cites 20 articles**, 1 of which can be accessed for free:  
<http://www.sciencemag.org/cgi/content/full/328/5984/1382#otherarticles>

This article appears in the following **subject collections**:  
Geochemistry, Geophysics  
[http://www.sciencemag.org/cgi/collection/geochem\\_phys](http://www.sciencemag.org/cgi/collection/geochem_phys)

range of fish  $\delta^{18}\text{O}$  values is translated into a temperature range of at least  $25^\circ\text{C}$ . Lécuyer *et al.* (26) have shown that the  $\delta^{18}\text{O}$  of the global ocean most likely ranged from  $-1$  to  $0\text{‰}$  [standard mean ocean water (SMOW) values] throughout the Jurassic and Cretaceous. Accordingly, the lowest temperatures of  $12^\circ \pm 2^\circ\text{C}$  correspond to the highest fish  $\delta^{18}\text{O}$  values approaching  $22\text{‰}$ , and the highest temperatures of  $36^\circ \pm 2^\circ\text{C}$  correspond to the lowest fish  $\delta^{18}\text{O}$  values close to  $18\text{‰}$  (Fig. 2). Ichthyosaurs and plesiosaurs have  $\delta^{18}\text{O}$  values similar to those of fish at a corresponding temperature range of  $26^\circ \pm 2^\circ\text{C}$  estimated from fish and seawater  $\delta^{18}\text{O}$  values of  $19.5\text{‰}$  and  $-1$  to  $0\text{‰}$ , respectively (Fig. 2). The regression line for mosasaurs intercepts the horizontal null line at a lower  $\delta^{18}\text{O}$  value of  $18.5\text{‰}$ , thus indicating a possible higher body temperature of  $30^\circ \pm 2^\circ\text{C}$ . These temperature ranges are the minimal values that can be considered for ichthyosaur, plesiosaur, and mosasaur body temperatures if the  $\delta^{18}\text{O}$  of their body equaled that of ambient seawater.

However, aquatic breathing vertebrates have body waters that are slightly  $^{18}\text{O}$ -enriched relative to ambient water in the absence of transcutaneous evapotranspiration, and published data for modern aquatic reptiles reveal that this isotopic enrichment does not exceed  $2\text{‰}$  (30, 31). Consequently, the body temperatures of studied ichthyosaurs and plesiosaurs could have been as high as  $35^\circ \pm 2^\circ\text{C}$  and even close to  $39^\circ \pm 2^\circ\text{C}$  for mosasaurs, according to Kolodny *et al.*'s equation (21). Both slope values of linear regressions and estimates of body temperatures are in good agreement with the swimming performances that were modeled for these three groups of marine reptiles. Massare (32, 33) and Motani (14) suggested that ichthyosaurs were pursuit predators, whereas most mosasaurs were ambush predators, not requiring high metabolic rates all the time. Plesiosaurs were considered to have been cruisers, although slower than ichthyosaurs in sustained speed.

The  $\delta^{18}\text{O}$  values of Mesozoic ichthyosaurs and plesiosaurs support the hypothesis that these large predators were able to regulate their body temperature independently of the surrounding water temperature even when it was as low as about  $12^\circ \pm 2^\circ\text{C}$ . In the case of mosasaurs, we cannot exclude the possibility that their body temperature was partly influenced by the temperature of ambient water. In any case, estimated body temperatures in the range from  $35^\circ \pm 2^\circ\text{C}$  to  $39^\circ \pm 2^\circ\text{C}$  encompass those of modern cetaceans (34) and suggest a high metabolic rate required for predation and fast swimming over large distances, especially in cold waters.  $\delta^{18}\text{O}$  data from tooth phosphate reveal the existence of homeothermy for ichthyosaurs and plesiosaurs, and of at least partial homeothermy for mosasaurs, with in all cases a taxonomic resolution that does not exceed the family or infraorder. These three distinct phylogenetic groups of large marine reptiles were able to maintain a body temperature substantially higher than that of ambient marine waters,

indicating that some kind of endothermy operated as an internal source of heat.

#### References and Notes

- A. F. Bennett, J. W. Hicks, A. J. Cullum, *Evolution* **54**, 1768 (2000).
- C. P. Hickman, L. S. Roberts, A. Larson, *Integrated Principles of Zoology* (McGraw-Hill Science, New York, 2000).
- J. K. Carlson, K. J. Goldman, C. G. Lowe, in *Biology of Sharks and Their Relatives*, J. C. Carrier, J. A. Musick, M. R. Heithaus, Eds. (CRC Press, Boca Raton, FL, 2004), pp. 203–224.
- F. V. Paladino, M. P. O'Connor, J. R. Spotila, *Nature* **344**, 858 (1990).
- M. E. Lutcavage, P. G. Bushnell, D. R. Jones, *Can. J. Zool.* **70**, 348 (1992).
- B. Heinrich, *Integr. Comp. Biol.* **29**, 1157 (1989).
- B. A. Block, J. R. Finnerty, A. F. Stewart, J. Kidd, *Science* **260**, 210 (1993).
- R. S. Seymour, *Plant Cell Environ.* **27**, 1014 (2004).
- V. De Buffrénil, J. Mazin, *Paleobiology* **16**, 435 (1990).
- R. S. Seymour, *Nature* **262**, 207 (1976).
- R. S. Seymour, C. L. Bennett-Stamper, S. D. Johnston, D. R. Carrier, G. C. Grigg, *Physiol. Biochem. Zool.* **77**, 1051 (2004).
- R. T. Bakker, *Nature* **238**, 81 (1972).
- P. Wellnhofer, *The Illustrated Encyclopedia of Pterosaurs* (Crescent Books, New York, 1991).
- R. Motani, *Paleobiology* **28**, 251 (2002).
- M. J. Benton, *Vertebrate Palaeontology* (Wiley-Blackwell, Oxford, 2005).
- R. Motani, *Nature* **415**, 309 (2002).
- J. Wiffen, V. De Buffrénil, A. De Ricqlès, J.-M. Mazin, *Geobios* **28**, 625 (1995).
- J. A. Massare, *J. Vertebr. Paleontol.* **7**, 121 (1987).
- B. P. Kear, *Cretac. Res.* **26**, 769 (2005).
- A. Longinelli, *Geochim. Cosmochim. Acta* **48**, 385 (1984).
- Y. Kolodny, B. Luz, O. Navon, *Earth Planet. Sci. Lett.* **64**, 398 (1983).
- Materials and methods are available as supporting material on Science Online.
- T. F. Anderson, B. N. Popp, A. C. Williams, L. Ho, J. D. Hudson, *J. Geol. Soc. London* **151**, 125 (1994).
- Y. Kolodny, B. Luz, in *Stable Isotope Geochemistry: A Tribute to Samuel Epstein*, H. P. Taylor, J. R. O'Neil, I. R. Kaplan, Eds. (Geochemical Society, University Park, St. Louis, MO, 1991), vol. 3, pp. 105–119.
- Y. Kolodny, M. Raab, *Palaeogeogr. Palaeoclimatol. Palaeoecol.* **64**, 59 (1988).
- C. Lécuyer *et al.*, *Paleoceanography* **18**, 1076 (2003).
- Z. D. Sharp, V. Atudorei, H. Furrer, *Am. J. Sci.* **300**, 222 (2000).
- A. Zazzo, C. Lécuyer, A. Mariotti, *Geochim. Cosmochim. Acta* **68**, 1 (2004).
- M. R. Wadley, G. R. De Oliveira, E. J. Rohling, A. J. Payne, *Global Planet. Change* **32**, 89 (2002).
- R. Amiot *et al.*, *Palaeogeogr. Palaeoclimatol. Palaeoecol.* **243**, 412 (2007).
- R. E. Barrick, A. G. Fischer, W. J. Showers, *Palaios* **14**, 186 (1999).
- J. A. Massare, *Paleobiology* **14**, 187 (1988).
- J. A. Massare, in *Mechanics and Physiology of Animal Swimming*, L. Maddock, Q. Bone, J. M. V. Rayner, Eds. (Cambridge Univ. Press, Cambridge, 1994), pp. 133–149.
- P. Morrison, *Biol. Bull.* **123**, 154 (1962).
- The authors thank M. Sander, B. McNab, and R. Seymour for preliminary discussions of these data during the workshop dedicated to "Sauropod gigantism" that was held in Bonn, Germany, in November 2008. We are also grateful to D. Brinkman and J. Gardner (Royal Tyrrell Museum), S. Etches and J. Clarke, G. Suan, J. Lindgren (Lund University), B. Kear (La Trobe University), and A. Schulp (Maastricht University) for providing samples. L. Simon and G. Escarguel helped us in the statistical treatment of data. This study was funded by both CNRS and the Institut Universitaire de France.

#### Supporting Online Material

www.sciencemag.org/cgi/content/full/328/5984/1379/DC1  
Materials and Methods  
Table S1

25 January 2010; accepted 28 April 2010  
10.1126/science.1187443

## Climate Change Will Affect the Asian Water Towers

Walter W. Immerzeel,<sup>1,2\*</sup> Ludovicus P. H. van Beek,<sup>2</sup> Marc F. P. Bierkens<sup>2,3</sup>

More than 1.4 billion people depend on water from the Indus, Ganges, Brahmaputra, Yangtze, and Yellow rivers. Upstream snow and ice reserves of these basins, important in sustaining seasonal water availability, are likely to be affected substantially by climate change, but to what extent is yet unclear. Here, we show that meltwater is extremely important in the Indus basin and important for the Brahmaputra basin, but plays only a modest role for the Ganges, Yangtze, and Yellow rivers. A huge difference also exists between basins in the extent to which climate change is predicted to affect water availability and food security. The Brahmaputra and Indus basins are most susceptible to reductions of flow, threatening the food security of an estimated 60 million people.

Mountains are the water towers of the world (1), including for Asia, whose rivers all are fed from the Tibetan plateau and adjacent mountain ranges. Snow and glacial melt are important hydrologic processes in these areas (2, 3), and changes in temperature

and precipitation are expected to seriously affect the melt characteristics (4). Earlier studies have addressed the importance of glacial and snow melt and the potential effects of climate change on downstream hydrology, but these are mostly qualitative (4–6) or local in nature (7, 8). The relevance of snow and glacial melt for Asian river basin hydrology therefore remains largely unknown, as does how climate change could affect the downstream water supply and food security.

We examined the role of hydrological processes in the upstream areas, which we defined as

<sup>1</sup>FutureWater, Costerweg 1G, 6702 AA Wageningen, Netherlands. <sup>2</sup>Department of Physical Geography, Utrecht University, Post Office Box 80115, Utrecht, Netherlands. <sup>3</sup>Deltares, Post Office Box 80015, 3508 TC Utrecht, Netherlands.

\*To whom correspondence should be addressed. E-mail: w.immerzeel@futurewater.nl

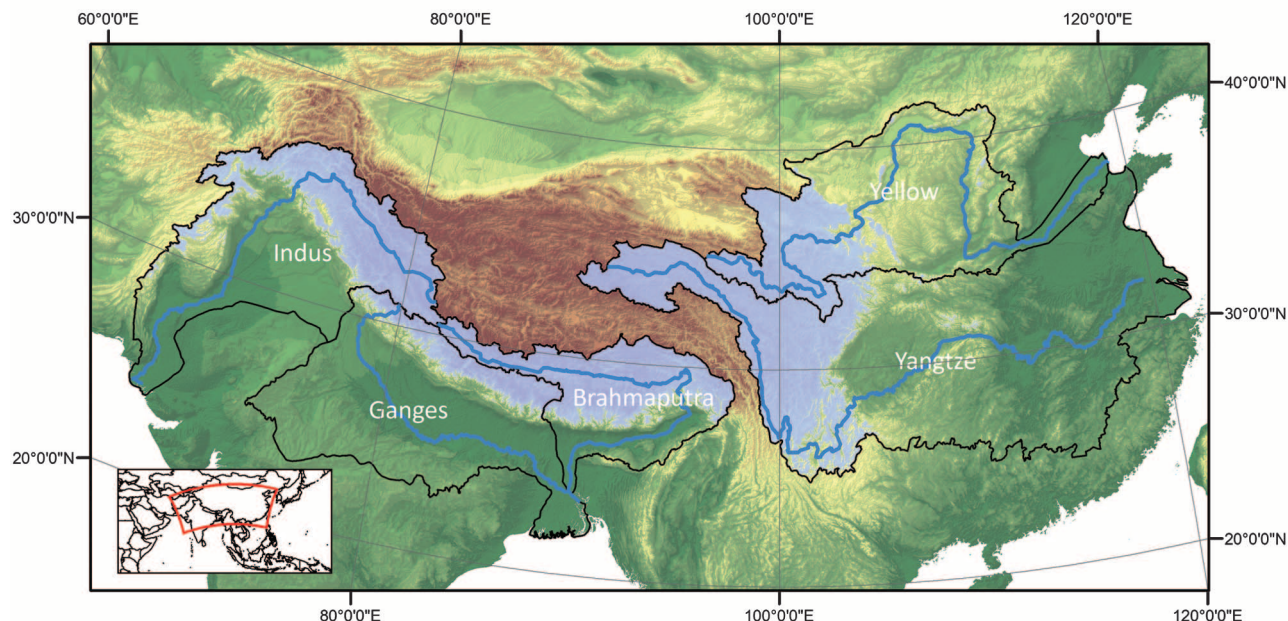


**Fig. 1.** Basin boundaries and river courses of the Indus, Ganges, Brahmaputra, Yangtze, and Yellow rivers. Blue areas denote areas with elevation exceeding 2000 masl. The digital elevation model in the background shows the topography ranging from low elevations (dark green) to high elevations (brown).

all areas higher than 2000 m above sea level (masl), on the water supply of the five major Southeast Asian basins (Fig. 1). These basins, which provide water to more than 1.4 billion people (over 20% of the global population), vary considerably in their characteristics (Table 1). The Yangtze has the largest population of the five basins, whereas the Ganges is the most densely populated. The Indus and Brahmaputra basins have extensive upstream areas (i.e., above 2000 m) and larger glaciated areas than the Yangtze and Yellow river basins (9). The Ganges, Brahmaputra and Yangtze basins are wetter than the Yellow and Indus basins (10). The Indus, Ganges, and Yangtze basins support large-scale irrigation systems (11) with high net irrigation water demand, but in the Indus the difference between basin precipitation and net irrigation demand is highest. We investigated three related components of these river basins: (i) the current importance of meltwater in overall river basin hydrology; (ii) observed cryospheric changes; and (iii) the effects of climate change on the water supply from the upstream basins and on food security.

We used the Normalized Melt Index (NMI) over the period 2001 to 2007 to quantify the importance of meltwater from the upstream areas on overall basin hydrology. NMI is defined as the volumetric snow and glacier upstream discharge divided by the downstream natural discharge. Upstream discharge is calculated with a calibrated snow melt runoff model (SRM) (12, 13). Downstream natural discharge is calculated by subtracting the natural evaporation ( $E_n$ ) of the basins, calculated with a hydrological model (14), from precipitation ( $P$ ) (15).  $E_n$  excludes additional evaporation from irrigated areas, because irrigation water is derived from upstream sources. The

**Table 1.** Characteristics of the five major Southeast Asian basins. Population data (2005) are based on the GPWv3 dataset [http://sedac.ciesin.columbia.edu/gpw (9 March 2009)]; precipitation data (average from 2001 to 2007) are based on (10); glacier areas are based on a dataset [http://glims.colorado.edu/glacierdata (9 March 2009)] provided by the Global Land Ice Measurements from Space (GLIMS) project (9). Irrigated areas and net irrigation water demand are based on (11). Upstream refers to the area > 2000 m.

Parameter	Indus	Ganges	Brahmaputra	Yangtze	Yellow
Total area (km <sup>2</sup> )	1,005,786	990,316	525,797	2,055,529	1,014,721
Total population (10 <sup>3</sup> )	209,619	477,937	62,421	586,006	152,718
Annual basin precipitation (mm)	423	1,035	1,071	1,002	413
Upstream area (%)	40	14	68	29	31
Glaciated area (%)	2.2	1.0	3.1	0.1	0.0
Annual upstream precipitation (%)	36	11	40	18	32
Annual downstream precipitation (%)	64	89	60	82	68
Irrigated area (km <sup>2</sup> )	144,900	156,300	5,989	168,400	54,190
Net irrigation water demand (mm)	908	716	480	331	525

difference  $P - E_n$  is therefore a measure of natural downstream discharge. The NMI is a more reliable measure than the commonly used meltwater fractions of total river discharge, which are affected by reservoirs, and water extractions (13). The great size of the basins that we analyze allows us to use melt parameters calculated for whole basins, rather than a different set of melt parameters for each different glacier, because each basin contains many glaciers of all types. Results from the NMI analysis (Fig. 2) indicate that for the present-day climate, meltwater plays an important role in the Indus and Brahmaputra river basins. This is most evident in the Indus: Discharge generated by snow and glacial melt is 151% of the total discharge naturally generated in the downstream areas. In the Brahmaputra basin this amounts to 27%. The contribution of snow and glacier water to the Ganges (10%), Yangtze (8%), and Yellow (8%) rivers is limited owing to comparatively large downstream

areas, limited upstream precipitation, smaller glaciers, and/or wet monsoon-dominated downstream climates (Table 1). In the Indus and Ganges basins, about 40% of the meltwater originates from glaciers, whereas in the other basins the glacial melt contribution is much less.

Since the end of the last ice age, an almost worldwide recession in glaciers has been observed (16), a trend that also applies to most of the glaciers in the Himalayas. Annual net imbalance rates of 0.5 to 0.9 m year<sup>-1</sup> have been observed from time series of digital elevation models in the Everest region in Nepal (17) and SPOT satellite imagery in the western Himalayas (18), whereas radioactivity analysis in ice cores revealed no net accumulation of ice in a high-elevation glacier in Tibet (19). However, there are some regional anomalies (13). We used the DMT-1 GRACE gravity model (20) in combination with derived precipitation trends (10) to identify large-scale

trends in snow and ice storage in each of the five basins. Results were inconclusive. We identified a negative trend of  $-0.22 \pm 0.05 \text{ m year}^{-1}$  only in the Ganges basin. A positive trend of  $0.19 \pm 0.02 \text{ m year}^{-1}$  was observed in the Indus basin, while in the other basins no discernible trends were identified (13). On the basis of this review, we conclude that there is a general decrease in the ice volumes of Asian basins, although regional anomalies exist and, as regional quantification of these trends is lacking, the uncertainty about these trends is substantial.

We made projections of future upstream discharge using a hydrological modeling approach that incorporates uncertainty about the cryospheric response by employing a scenario analysis. The hydrological model SRM simulated the present-day discharge with acceptable accuracy (fig. S1). To provide a multimodel assessment of future water availability from the upstream river basins, we forced the SRM model with outputs from five general circulation models (GCMs) for the SRES A1B scenario over the period 2046 to 2065. In addition, two different scenarios of future glacier

size were modeled (13): (i) a best guess based on glacier mass-balance calculations assuming trends in degree days and snowfall between current time and 2050 (calculated by the GCMs) to be linear, and (ii) an extreme (and unlikely) scenario with total disappearance of all glaciers to serve as a reference.

Upstream water supply is crucial to sustain upstream reservoir systems, which are used to store and release water to downstream areas when most needed. Irrigation water for the Indus Basin Irrigation Systems, which is the largest irrigation network in the world, is, for example, regulated through two major storage dams (Tarbela dam on the Indus River and the Mangla dam on the Jhelum River). Both are located in the upper Indus basin and are fed predominantly by meltwater. Any change in upstream water supply to these dams will have a profound effect on millions of people downstream. Our results show a substantial variation in changes in future water supply (Fig. 3). The best-guess glacier scenario resulted in a modeled decrease in mean upstream water supply from the upper Indus ( $-8.4\%$ ), the Ganges ( $-17.6\%$ ), Brahmaputra ( $-19.6\%$ ), and Yangtze rivers ( $-5.2\%$ ). Although these changes are considerable, they are less than the decrease in meltwater production would suggest, because this reduction is partly compensated for by increased mean upstream rainfall (Indus  $+25\%$ , Ganges  $+8\%$ , Brahmaputra  $+25\%$ , Yangtze  $+5\%$ , Yellow  $+14\%$ ). The analysis even shows a notable 9.5% increase in upstream water yield in the Yellow River because this basin depends only marginally on glacial melt (Fig. 2). Results should be treated with caution, however, because most climate models have difficulty simulating mean monsoon and the interannual precipitation variation (21, 22), despite recent progress in improving the resolution of anticipated spatial and temporal changes in precipitation. Nevertheless, we conclude that although considerable cryospheric changes are to be expected, their impact will be less than anticipated by, for example, the 4AR of the Intergovernmental Panel on Climate Change (IPCC) (2). In that report, it was suggested that the current trends of glacier melt and potential climate change may cause the Ganges, Indus, Brahmaputra, and other rivers to become seasonal rivers in the near future. We argue that these rivers already are seasonal rivers, because the melt and rain seasons generally coincide and a decrease in meltwater is partially compensated for by an increase in precipitation. Figure 3 also shows a temporal shift in the upstream hydrograph patterns. The Yellow River, in particular, shows a consistent increase in early spring discharge. This is highly beneficial because most reservoirs are empty at the beginning of the growing season. An accelerated melt peak may thus alleviate a shortage of irrigation water in the drought-prone early stages of the growing season. In addition, further temporal shifts in the hydrograph could occur as a result of changes in seasonal glacier storage caused by a reduced glacier area (23).

**Fig. 2.** Normalized melt index (NMI) for snow and glacier melt for the present (2000 to 2007) climate.

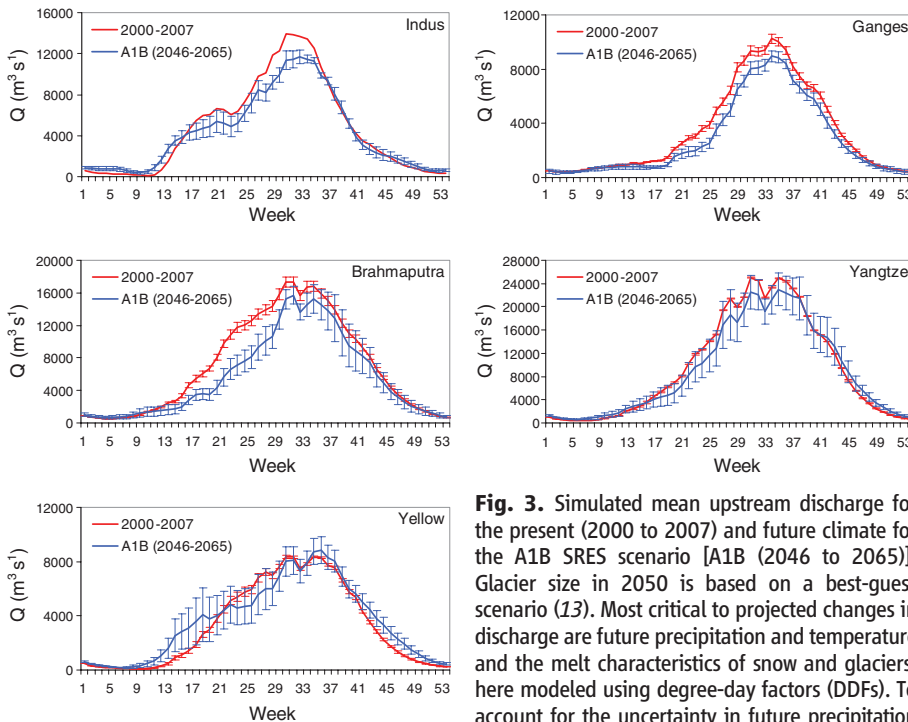
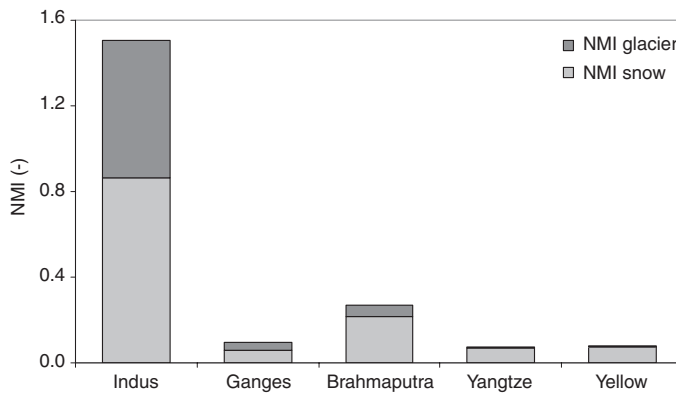


**Fig. 3.** Simulated mean upstream discharge for the present (2000 to 2007) and future climate for the A1B SRES scenario [A1B (2046 to 2065)]. Glacier size in 2050 is based on a best-guess scenario (13). Most critical to projected changes in discharge are future precipitation and temperature and the melt characteristics of snow and glaciers, here modeled using degree-day factors (DDFs). To account for the uncertainty in future precipitation and temperature, the best-guess scenario was run

with five different GCMs (CCMA-CGCM3, GFDL-CM2, MPIM-ECHAM5, NIES-MIROC3, UKMO-HADGEM1). For the upper Indus basin, the ice and snow DDFs are constrained by observed runoff. No runoff observations were available for the other upper basins so that DDFs from the Indus were used. To account for this additional uncertainty, we performed a first-order-second-moment analysis (13). Vertical error bars ( $\pm 1\sigma$ ) from the Indus thus include only the uncertainty about future climate, whereas the projected discharge of the other basins includes uncertainty about both future climate as well as basin-specific DDFs (assumed Gaussian with mean snow DDF =  $4 \text{ mm } ^\circ\text{C}^{-1} \text{ day}^{-1}$ , mean ice DDF =  $7 \text{ mm } ^\circ\text{C}^{-1} \text{ day}^{-1}$ , and both with  $\sigma = 1 \text{ mm } ^\circ\text{C}^{-1} \text{ day}^{-1}$ ). Vertical error bars around present discharge are due to uncertainty about snow and ice DDFs only.

Regardless of the compensating effects of increased rainfall in the two basins with the largest NMI, the Indus and the Brahmaputra, summer and late spring discharges are eventually expected to be reduced consistently and considerably around 2046 to 2065 after a period with increased flows due to accelerated glacial melt. Figure S2 also shows the extreme scenario in which all glaciers are assumed to have disappeared. Again, the Indus and Brahmaputra show the most pronounced changes.

These anticipated changes will also have considerable effects on food security. By relating changes in upstream water availability to net irrigation requirements (11), observed crop yields, caloric values of the crops, and required human energy consumption, one can estimate the change in the number of people that can be fed (13). The results (based on a best guess of 2050 glacier area) show a sizable difference between the five basins. Estimates range from a decrease of  $-34.5 \pm 6.5$  million people that can be fed in the Brahmaputra basin to  $-26.3 \pm 3.0$  million in the Indus basin,  $-7.1 \pm 1.3$  million in the Yangtze basin, and  $-2.4 \pm 0.2$  million in the Ganges basin, and an increase of  $3.0 \pm 0.6$  million in the Yellow River basin. In total, we estimate that the food security of 4.5% of the total population will be threatened as a result of reduced water availability. The strong need for prioritizing adaptation options and further increasing water productivity is therefore ever more eminent (24). Figure S3 shows the projected changes in food security for the two different glacier scenarios. The difference between the scenarios is largest for the Indus and Brahmaputra basins, as a direct result of the high

NMI in these areas. Clearly, upstream discharge and downstream food security of the Indus and Brahmaputra basins are the most sensitive to climate change.

We conclude that Asia's water towers are threatened by climate change, but that the effects of climate change on water availability and food security in Asia differ substantially among basins and cannot be generalized. The effects in the Indus and Brahmaputra basins are likely to be severe owing to the large population and the high dependence on irrigated agriculture and meltwater. In the Yellow River, climate change may even yield a positive effect as the dependence on meltwater is low and a projected increased upstream precipitation, when retained in reservoirs, would enhance water availability for irrigated agriculture and food security.

#### References and Notes

1. D. Viviroli, H. H. Dürr, B. Messerli, M. Meybeck, R. Weingartner, *Water Resour. Res.* **43**, W07447 (2007).
2. R. V. Cruz *et al.*, in *Climate Change 2007: Impacts, Adaptation and Vulnerability. Contribution of Working Group II to the Fourth Assessment Report of the Intergovernmental Panel on Climate Change*, M. L. Parry *et al.*, Eds. (Cambridge Univ. Press, Cambridge and New York, 2007).
3. W. W. Immerzeel, P. Droogers, S. M. de Jong, M. F. P. Bierkens, *Remote Sens. Environ.* **113**, 40 (2009).
4. T. P. Barnett, J. C. Adam, D. P. Lettenmaier, *Nature* **438**, 303 (2005).
5. B. C. Bates, Z. W. Kundzewicz, S. Wu, J. P. Palutikof, Eds., *Climate Change and Water* (IPCC, Geneva, 2008).
6. D. Cyranski, *Nature* **438**, 275 (2005).
7. P. Singh, L. Bengtsson, *J. Hydrol.* **300**, 140 (2005).
8. H. G. Rees, D. N. Collins, *Hydrol. Process.* **20**, 2157 (2006).
9. B. H. Raup *et al.*, *Global Planet. Change* **56**, 101 (2007).

10. G. J. Huffman *et al.*, *J. Hydrometeorol.* **8**, 38 (2007).
11. S. Siebert *et al.*, *Hydrol. Earth Syst. Sci.* **9**, 535 (2005).
12. J. Martinec, *Nord. Hydrol.* **6**, 145 (1975).
13. Materials and methods and discussion are available as supporting material on Science Online.
14. M. F. P. Bierkens, L. P. H. van Beek, *J. Hydrometeorol.* **10**, 953 (2009).
15. T. D. Mitchell, P. D. Jones, *Int. J. Climatol.* **25**, 693 (2005).
16. R. G. Barry, *Prog. Phys. Geogr.* **30**, 285 (2006).
17. T. Bolch, M. F. Buchroithner, T. Pieczonka, A. Kunert, *J. Glaciol.* **54**, 592 (2008).
18. E. Berthier *et al.*, *Remote Sens. Environ.* **108**, 327 (2007).
19. N. M. Kehrwald *et al.*, *Geophys. Res. Lett.* **35**, L22503 (2008).
20. E. Klees *et al.*, *Geophys. J. Int.* **175**, 417 (2008).
21. H. Annamalai, K. Hamilton, K. R. Sperber, *J. Clim.* **20**, 1071 (2007).
22. S. Yang *et al.*, *J. Clim.* **21**, 3755 (2008).
23. P. Jansson, R. Hock, T. Schneider, *J. Hydrol. (Amst.)* **282**, 116 (2003).
24. D. B. Lobell *et al.*, *Science* **319**, 607 (2008).
25. This study was financially supported by the Netherlands Organisation for Scientific Research (NWO) through a CASIMIR grant (018 003 002) and by the European Commission (Call FP7-ENV-2007-1 grant 212921) as part of the CEOP-AEGIS project ([www.ceop-aegis.org/](http://www.ceop-aegis.org/)) coordinated by the Université de Strasbourg. We thank P. Ditmar (Department of Earth Observation and Space Systems, Technical University of Delft) for assistance with the GRACE trend analysis.

#### Supporting Online Material

[www.sciencemag.org/cgi/content/full/328/5984/1382/DC1](http://www.sciencemag.org/cgi/content/full/328/5984/1382/DC1)

Materials and Methods

SOM Text

Figs. S1 to S4

Table S1

References

12 October 2009; accepted 6 May 2010

10.1126/science.1183188

## Periodic, Chaotic, and Doubled Earthquake Recurrence Intervals on the Deep San Andreas Fault

David R. Shelly

Earthquake recurrence histories may provide clues to the timing of future events, but long intervals between large events obscure full recurrence variability. In contrast, small earthquakes occur frequently, and recurrence intervals are quantifiable on a much shorter time scale. In this work, I examine an 8.5-year sequence of more than 900 recurring low-frequency earthquake bursts composing tremor beneath the San Andreas fault near Parkfield, California. These events exhibit tightly clustered recurrence intervals that, at times, oscillate between  $\sim 3$  and  $\sim 6$  days, but the patterns sometimes change abruptly. Although the environments of large and low-frequency earthquakes are different, these observations suggest that similar complexity might underlie sequences of large earthquakes.

The idea that fault segments rupture in similar quasi-periodic earthquakes is a model increasingly incorporated into earthquake forecasts (1, 2). In certain places,

however, large systematic deviations from average recurrence intervals (3, 4) call into question the utility of this simple model. Examples of complex earthquake recurrence include chaotic intervals as well as period doubling, which is usually transitional between periodic and chaotic behavior (5, 6).

Numerical models sometimes show complexity in earthquake recurrence intervals, such as chaotic behavior and period doubling, in addition to periodic slip (7–13). Laboratory studies have also demonstrated evidence for complexity in frictional sliding experiments, especially near the transition from stable sliding (fault creep) to stick-slip (earthquakes) (5, 9, 14). Large natural earthquakes may be subject to similar controls, with fault interactions accounting for variations in recurrence intervals on a given fault segment (15, 16), but tens to hundreds of years between large events on a given natural fault strongly limit the number of observable intervals. Even in rare instances where long records exist, such as Nankai Trough, Japan (16), a 1300-year record of eight events on a given segment probably does not reveal the full variability of earthquake rupture. Likewise, the timing of the 2004 moment magnitude ( $M_w$ ) 6.0 Parkfield, California earthquake was not anticipated based on this segment's history of six prior earthquakes dating back to 1857 (17).

Smaller earthquakes, with correspondingly shorter recurrence times, provide a more tractable natural laboratory for investigating recurrence behavior. In this study, I examined the recurrence intervals of a “family” of similar low-frequency

U.S. Geological Survey, Menlo Park, CA 94025, USA. E-mail: dshelly@usgs.gov

## ERRATUM

Post date 30 July 2010

**Reports:** "Climate change will affect the Asian water towers" by W. W. Immerzeel *et al.* (11 June, p. 1382). In Fig. 3, the superscript minus signs in the units along the y axis were mistakenly omitted. The units should have read  $Q$  ( $\text{m}^3 \text{s}^{-1}$ ). The corrected figure is shown here.

